

## **Supporting Information for:**

### **Spontaneous Polarization Switching and Piezoelectric Enhancement of PVDF through Strong Hydrogen Bonds Induced by Layered Double Hydroxides**

Rui Tian,<sup>a</sup> Qi Xu,<sup>a</sup> Chao Lu,<sup>\*a</sup> Xue Duan,<sup>a</sup> Ren-gen Xiong<sup>b</sup>

<sup>a</sup>*State Key Laboratory of Chemical Resource Engineering, Beijing University of Chemical  
Technology, Beijing 100029, China*

<sup>b</sup>*Ordered Matter Science Research Center, Southeast University, Nanjing 211189, China*

## Experimental Section

**Materials.** Analytical-grade chemicals including N, N-dimethylformamide (DMF),  $\text{Co}(\text{NO}_3)_2 \cdot 6\text{H}_2\text{O}$ ,  $\text{Al}(\text{NO}_3)_3 \cdot 9\text{H}_2\text{O}$ ,  $\text{NaNO}_3$  and  $\text{NaOH}$  were purchased from Aladdin Chemical. Co. Ltd. Poly(vinylidene fluorid) was purchased from sigma-aldrich. PDMS and curing agents were purchased from Sylgard 184.

**Synthesis of ultrathin CoAl-CO<sub>3</sub>-LDHs.** The ultrathin LDHs were prepared as a modification of previously reported method,<sup>1</sup> and N, N-dimethylformamide (DMF) was employed as inhibitor for the growth of LDHs in Z-direction. Briefly,  $\text{NaNO}_3$  (0.1 mmol, 5 mL) was dissolved in the mixture of  $\text{H}_2\text{O}$  (7.7 mL) and DMF (2.3 mL), and the solution was added into flask at 80 °C. Simultaneously, 10 mL aqueous solution A containing  $\text{Co}(\text{NO}_3)_2 \cdot 6\text{H}_2\text{O}$  (0.2 mmol),  $\text{Al}(\text{NO}_3)_3 \cdot 6\text{H}_2\text{O}$  (0.1 mmol) and 9 mL aqueous solution B containing 0.09 g  $\text{NaOH}$  were added into the flask under continuous stirring at 80 °C. The suspension was stirred for another 5 min, and then centrifuged, washed with water for three times. The prepared LDHs were dispersed in DMF for further use.

**Preparation of PVDF-LDHs composites.** LDHs suspension at different concentrations (0.14, 0.28, 0.42, 0.56 and 0.7 mg/mL) were prepared in DMF. The PVDF-LDH composite films were fabricated by adding LDHs (5 mL) into PVDF (dissolved in DMF, 10g/L for 5 mL) dropwise, and the mixture was stirred for 2 h and finally dried at 120 °C for 4h (Scheme S1). The loading contents of LDHs in composites were calculated by the ratio of the loading amount of LDHs to the total amount of PVDF: 1.4, 2.8, 4.2, 5.6, and 7.0 wt% and labeled as PVDF-1.4%LDHs, PVDF-2.8%LDHs, PVDF-4.2%LDHs, PVDF-5.6%LDHs, and PVDF-7.0%LDHs, respectively. Pure PVDF film was fabricated under the same condition as a reference. Moreover, the ultrathin PVDF and PVDF-5.6%LDH films

were fabricated by spin-coating the PVDF and PVDF-5.6%LDH composites on ITO glass, followed by thermal treatment on heating stage of 120 °C. The as-prepared ultrathin films were for microcosmic ferroelectric measurements.

**Fabrication of piezoelectric nanogenerator.** The piezoelectric devices were fabricated by attaching conducting carbon electrodes and leads on top and bottom of the as-prepared films for an electrode-PVDF film-electrode stack. This stack was then encapsulated with PDMS (mixing with curing agents at the ratio of 10:1 and solidified at 80 °C) to avoid the interference of environment and enhance the robustness for the piezoelectric device.

The pressure imposed on the device was calculated by a physical model and followed the law of conservation of momentum:<sup>2</sup>

$$mgh = \frac{1}{2}mv^2$$

$$(F - mg)\Delta t = mv$$

$$P = \frac{F}{A}$$

Therefore, the  $m$  stands for the mass of the heavy object provide external force,  $h$  is the height where the object falls,  $A$  is the approximate active area (area under the external pressure), the  $\Delta t$  stands for the estimated average time difference (the time between the two consecutive voltage peak minus the falling and lifting time, 0.1 s), and  $g = 9.80$  N/kg. Thus, the pressure  $P$  can be calculated as 39 kPa.

The bending measurements were carried out to measure the sensitivity of the devices. Therefore, the tensile strain ( $\varepsilon$ ) of the thin film is approximately developed in the thickness direction ( $\varepsilon$ , parallel to the dipole orientation) during bending of the device into arc shape.

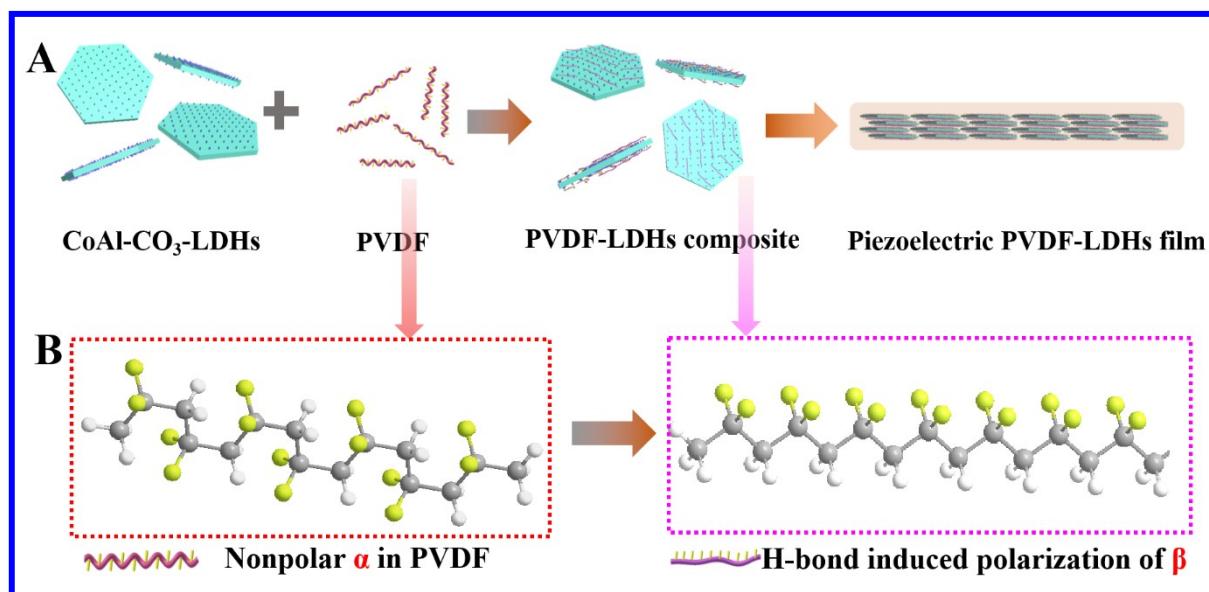
$$R.2\theta = L_0$$

$$\sin\theta = \sin\frac{L_0}{2R} = \frac{L}{2R}$$

$$\varepsilon = \frac{h}{2R}$$

According to the equation, the calculated tensile strain of PVDF-5.6%LDH thin film is ~0.25%, where,  $R$  (10 mm) is the bending radius and  $h$  is the thickness of the film (~50  $\mu\text{m}$  obtained from SEM side-view images).

**Sample Characterizations.** FT-IR spectra of flexible films were recorded on a Nicolet 6700 (Thermo Electron) with ZnSe crystal for the attenuated total reflection of the films; while FT-IR for the drop-coated thin films on ITO were recorded on Nicolet 8700 with DIGS TEC detector. X-ray diffraction (XRD) patterns of the LDHs and composite films were recorded using a Rigaku 2500 VB2 + PC diffractometer under the conditions: 40 kV, 50 mA, Cu K radiation (= 0.1541 nm) in the range from 10° to 40°. Atomic force microscopy (AFM) in tapping mode was carried out on a NanoScope IIIa (Digital Instruments Co., Santa Barbara, CA, USA) instrument. Transmission electron microscope (TEM) images were recorded on JEOL JEM-3010 with the accelerating voltage of 100 kV. The morphologies of films were investigated by a scanning electron microscope (Hitachi S-3500) and the accelerating voltage applied was 20 kV. Dielectric constants and dielectric loss of films with temperature dependencies and frequency dependencies were measured in the heating mode at 500–1M Hz. The electrical output voltages of films were recorded by a nanovoltmeter (rigol ds1204B), and the shortcut circuit current was measured by KEITHLEY 2450 sourcemeter and analyzed by kickstart accessory. PFM measurements were conducted on Atomic Force Microscopes (Asylum Research MFP-3D and Brucker Multimode 8).<sup>4</sup>



**Scheme S1.** (A) Schematic representation for the fabrication process for PVDF- LDH composite film, and (B) configuration rearrangement of PVDF.

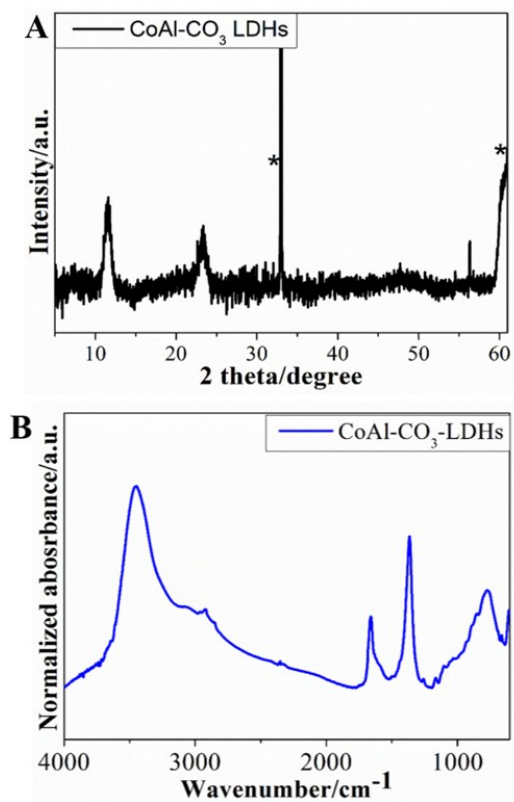


**Fig. S1** (A) XRD pattern and (B) FT-IR spectrum of LDHs.

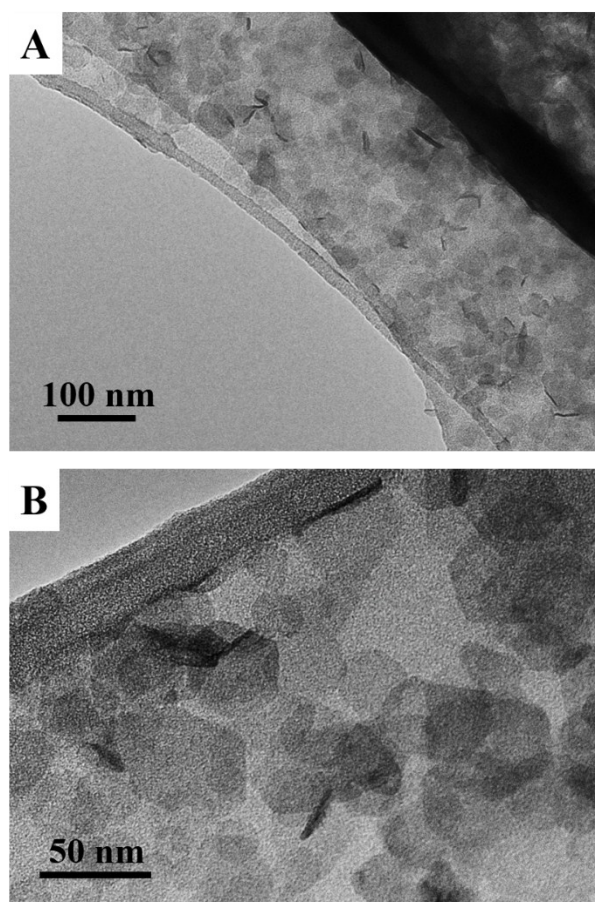


**Fig. S2** TEM images of LDHs.

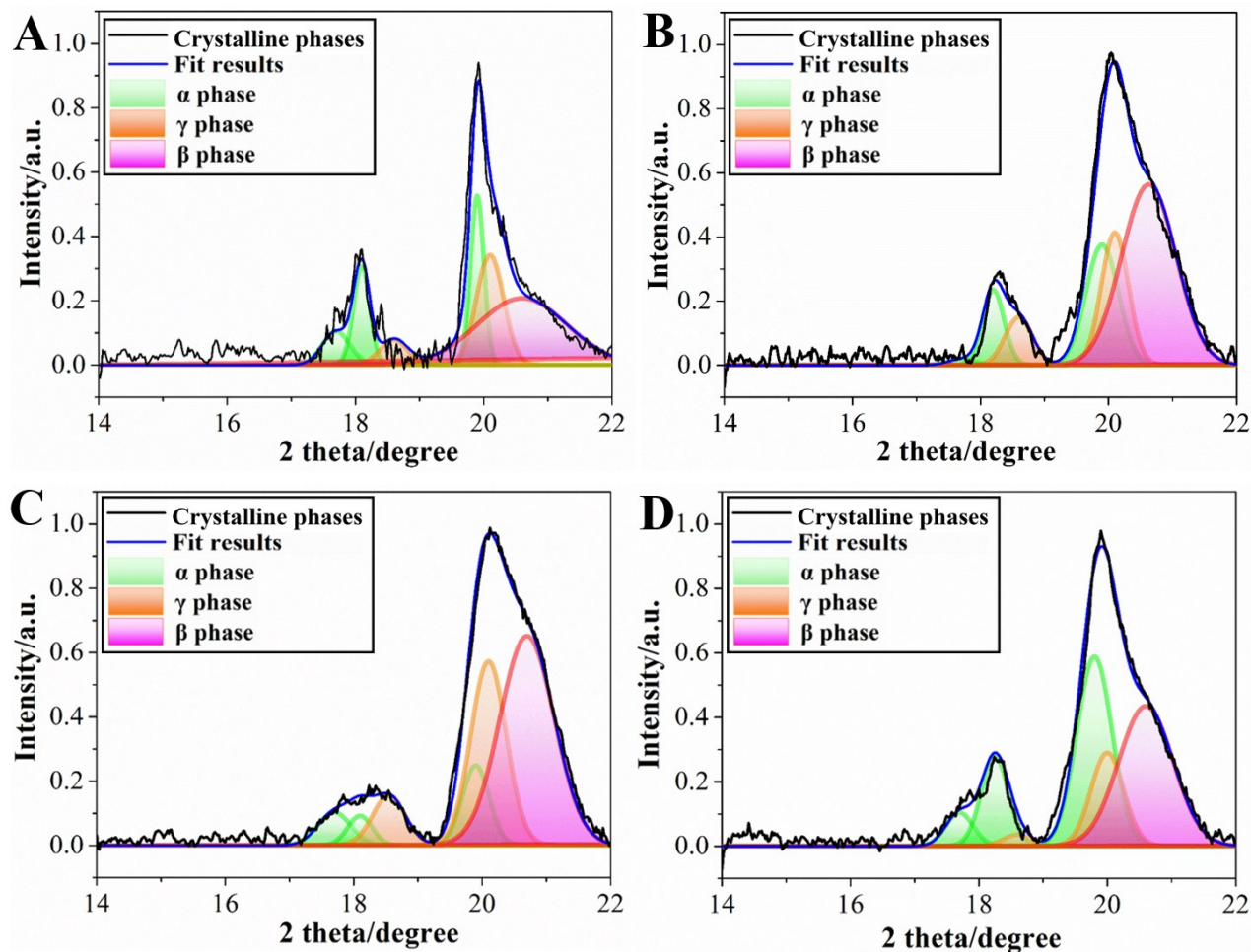


**Fig. S3** XRD patterns and fit results of PVDF- $x\%$ LDH composite films, from A to D:  $x\%$ =1.4%, 2.8%, 4.2% and 7%.

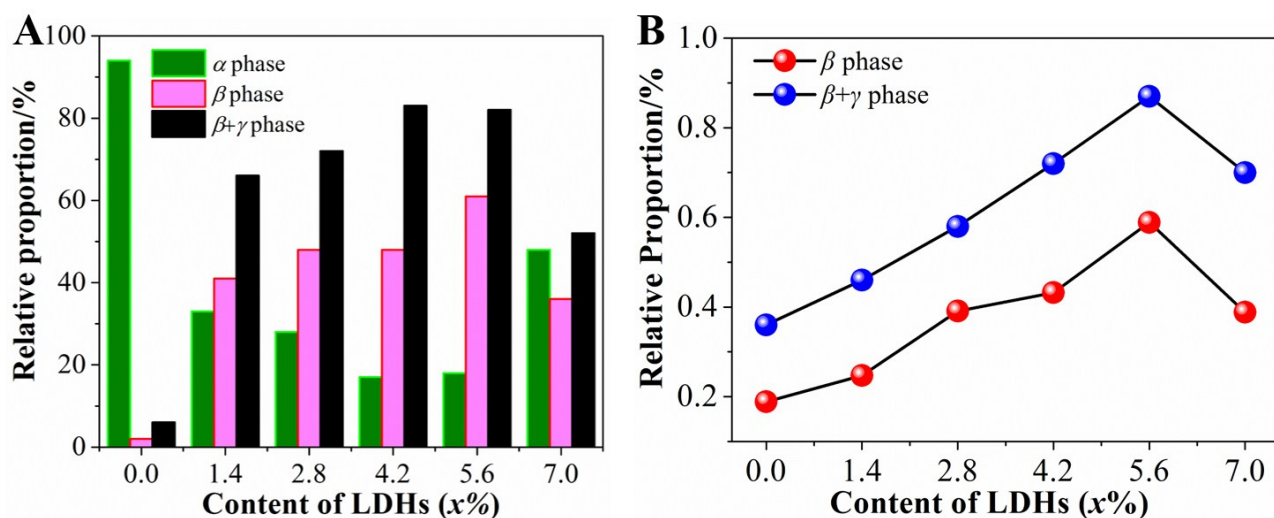


**Fig. S4** Analysis of phase contents in PVDF- $x\%$ LDH composite films for (A) XRD and (B) normalized IR absorbance results, content of LDHs ranges from 0%, 1.4%, 2.8%, 4.2%, 5.6%, to 7%.

The relative proportions of polar phases in PVDF- $x\%$ LDH composite films were calculated from the following equation<sup>5</sup>:

$$F(\beta, \gamma) = \frac{I_{\beta, \gamma}}{(K_{841}/K_{763})I_{763} + I_{\beta, \gamma}}$$

Where  $I_{764}$  and  $I_{\beta, \gamma}$  are the absorbance at 764 and 841  $\text{cm}^{-1}$ , and  $K_{764}$  and  $K_{\beta, \gamma}$  are the absorption coefficients, respectively. Furthermore, the curve deconvolution of the 841  $\text{cm}^{-1}$  band have been carried out to analyze the detailed content of  $\beta$  and  $\gamma$  phases:

$$F(\beta) = F_{\beta, \gamma} \times \left( \frac{A_{\beta}}{A_{\beta} + A_{\gamma}} \right) \times 100\%$$

$$F(\gamma) = F_{\beta, \gamma} \times \left( \frac{A_{\gamma}}{A_{\beta} + A_{\gamma}} \right) \times 100\%$$

where,  $A_{\beta}$  and  $A_{\gamma}$  are the integrated areas under the  $\beta$ - and  $\gamma$ - marked deconvoluted curves.

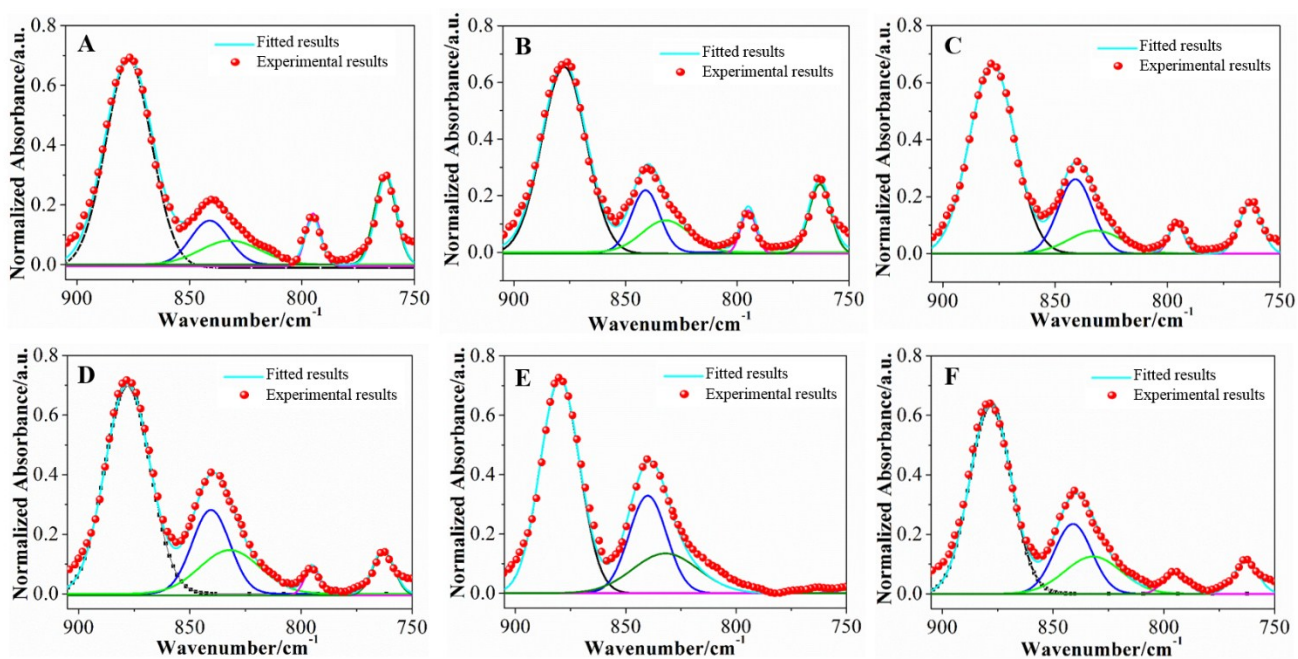


**Fig. S5** IR spectra of PVDF-*x*%LDH composite films in 915–750  $\text{cm}^{-1}$  wavenumber region to deconvolute the 841  $\text{cm}^{-1}$  band and to quantify exclusively the presence of  $\beta$ - and  $\gamma$ -phases: from A to F, the content of LDHs ranges from 0%, 1.4%, 2.8%, 4.2%, 5.6%, to 7%.

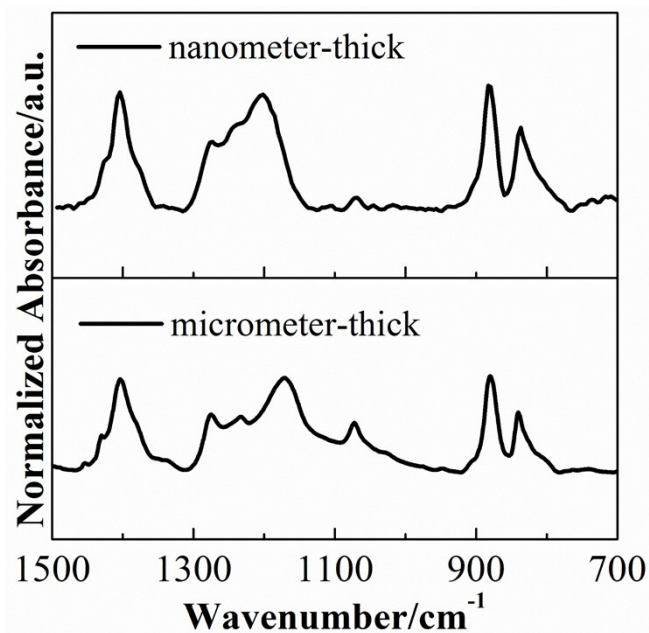


**Fig. S6** Normalized IR absorbance results of PVDF-5.6%LDH composite films fabricated by spin-coating (upper, nanometer-thick) and solution-casting (lower, micrometer-thick) methods in the range 700–1500 cm<sup>-1</sup>.

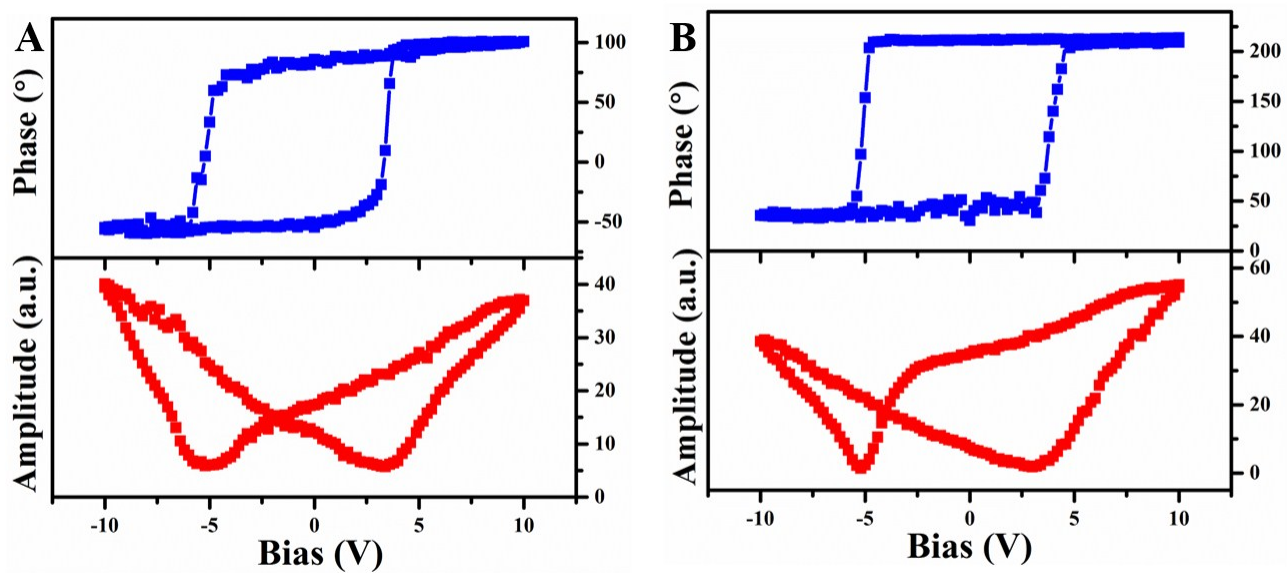


**Fig. S7** Comparison of hysteresis loops (blue) and the characteristic butterfly loops (red) for (A) PVDF and (B) PVDF-5.6%LDH composite films.

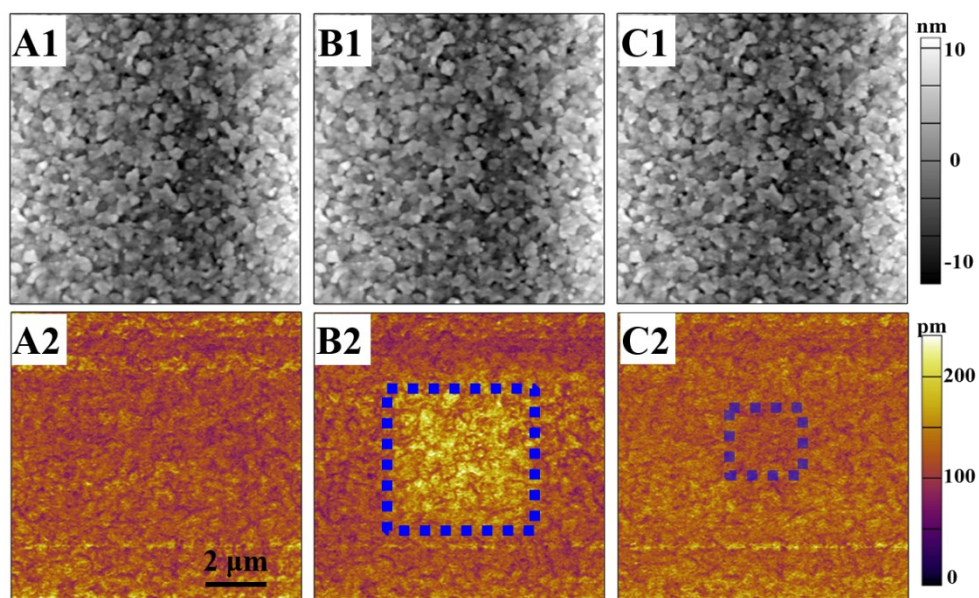


**Fig. S8** Polarization reversal measurements for PVDF film: the corresponding topographic images (top) and vertical piezoresponse images (bottom) of the film surface were achieved for (A) initial state, (B) after the first switching by scanning with the tip bias of  $-10$  V, and (C) after the back-switching by scanning with the tip bias of  $+10$  V.

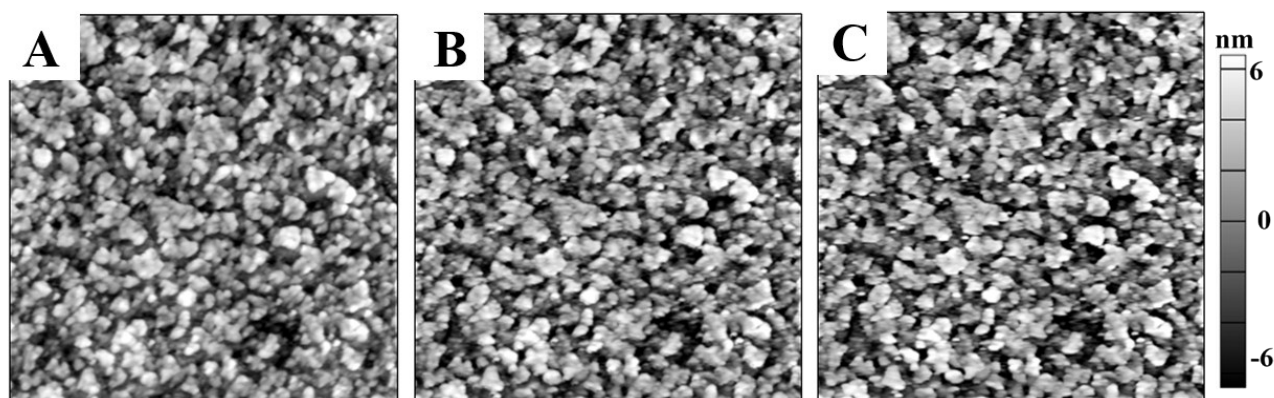


**Fig. S9** Polarization reversal measurements for PVDF-5.6%LDH film: the corresponding topographic images of the film surface were achieved for (A) initial state, (B) after the first switching by scanning with the tip bias of  $-10$  V, and (C) after the back-switching by scanning with the tip bias of  $+10$  V.

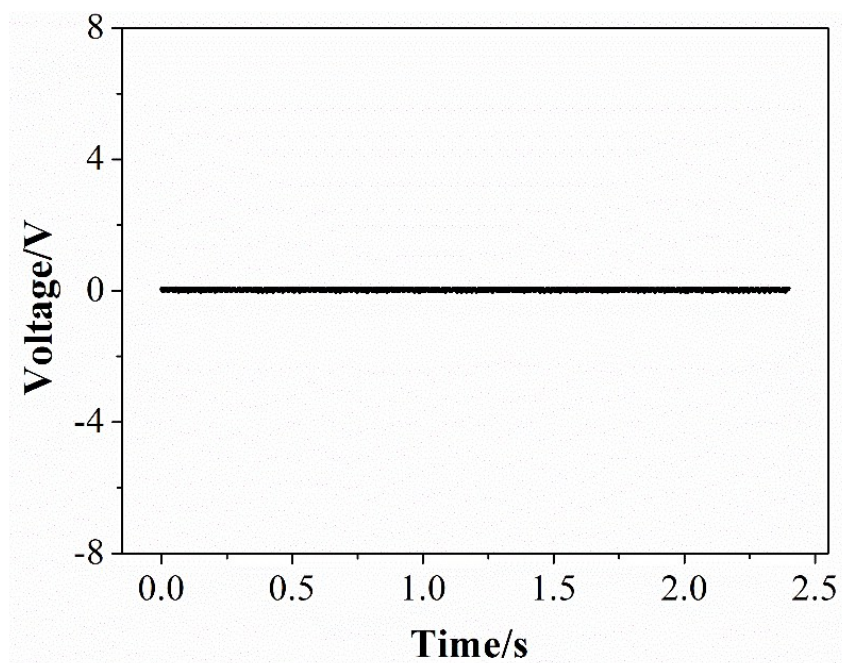


**Fig. S10** The generated output voltage for blank PDMS under impacting of 39 kPa pressure.

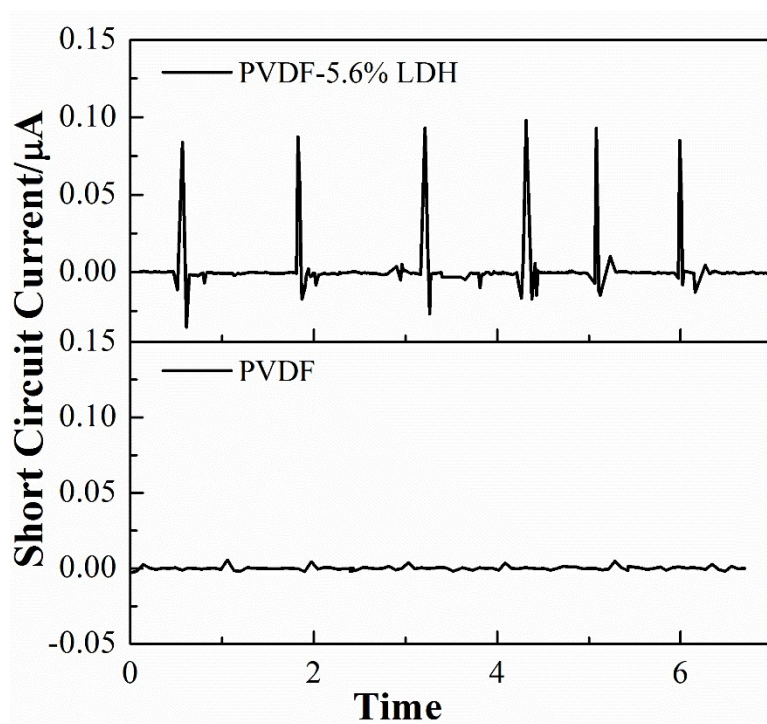


**Fig. S11** The generated short circuit current of PVDF and PVDF-5.6%LDH composite under impacting of 39 kPa.

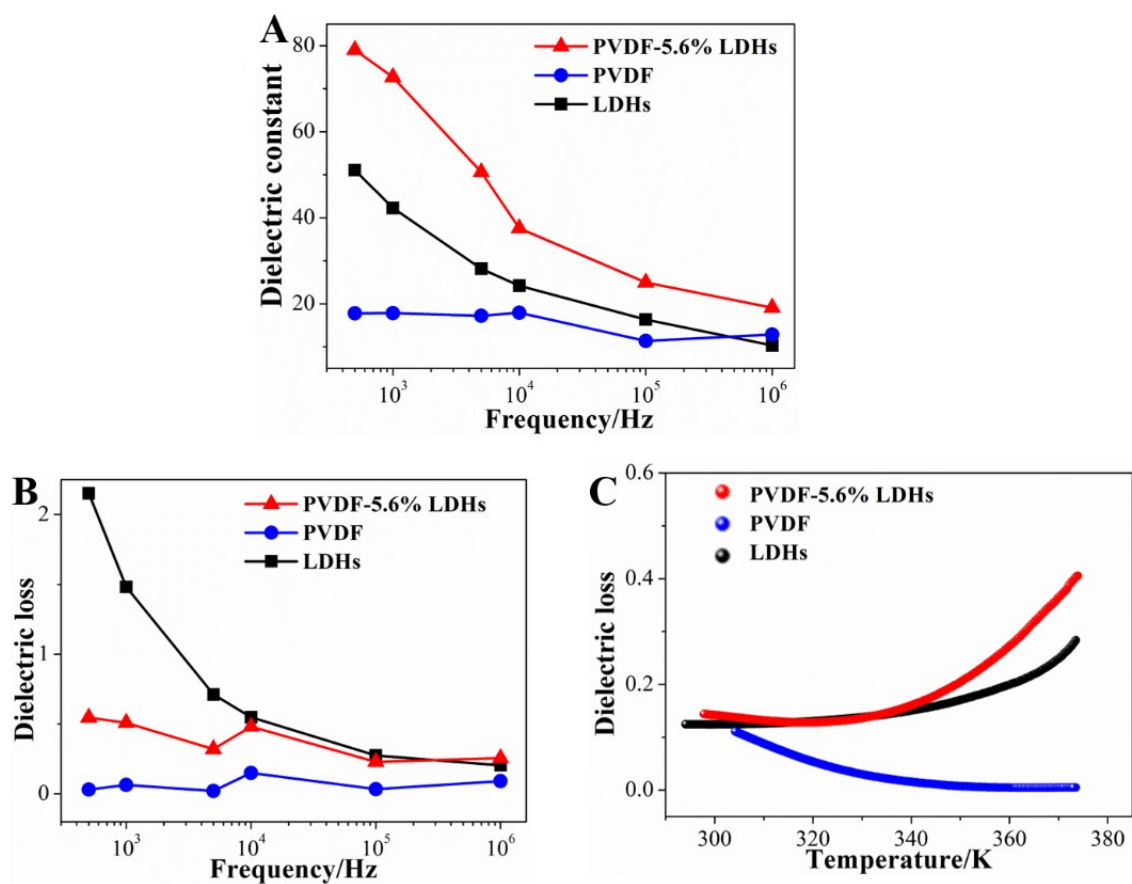


**Fig. S12** (A) Frequency-dependencies of dielectric constants measured at 30 °C; (B) frequency-dependencies (measured at 30 °C) and (C) temperature-dependencies (measured at 1M Hz) of dielectric loss for PVDF, LDHs and PVDF-5.6%LDH composite.

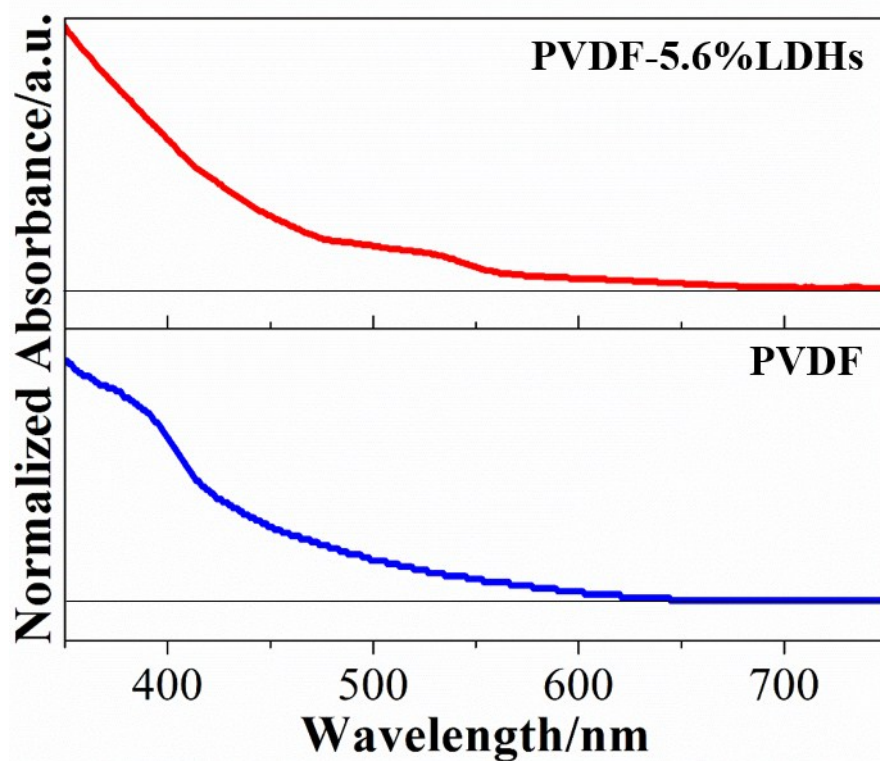


Fig. S13 UV absorption spectra of PVDF and PVDF-5.6%LDH composite.

References:

- 1 J. Yu, B. R. Martin, A. Clearfield, Z. Luo and L. Sun, *Nanoscale*, 2015, **7**, 9448.
- 2 (a) S. K. Karan, R. Bera, S. Paria, A. K. Das, S. Maiti, A. Maitra and B. B. Khatua, *Adv. Energy Mater.*, 2016, **6**, 1601016. (b) S. K. Karan, D. Mandal and B. B. Khatua, *Nanoscale*, 2015, **7**, 10655.
- 3 (a) K. I. Park, S. Xu, Y. Liu, G. T. Hwang, S. J. Kang, Z. L. Wang and K. J. Lee, *Nano Lett.*, 2010, **10**, 4939. (b) S. K. Ghosh, A. Biswas, S. Sen, C. Das, K. Henkel, D. Schmeisser and D. Mandal, *Nano Energy*, 2016, **30**, 621. (c) S. K. Ghosh, T. K. Sinha, B. Mahanty and D. Mandal, *Energy Technology*, 2015, **3**, 1190.
- 4 (a) Y. Zhang, Y. Liu, H. Y. Ye, D. W. Fu, W. Gao, H. Ma, Z. Liu, Y. Liu, W. Zhang, J. Li, G. L. Yuan, R. G. Xiong, *Angew. Chem. Int. Ed.*, 2014, **53**, 5064. (b) H. Y. Ye, W. Q. Liao, C. L. Hu, Y. Zhang, Y. M. You, J. G. Mao, P. F. Li, R. G. Xiong, *Adv. Mater.*, 2016, **28**, 2579.
- 5 (a) S. K. Ghosh, W. Rahman, T. R. Middy, S. Sen and D. Mandal, *Nanotechnology*, 2016, **27**, 215401; (b) B. S. Ince-Gunduz, R. Alpern, D. Amare, J. Crawford, B. Dolan, S. Jones, R. Kobylarz, M. Reveley and P. Cebe, *Polymer*, 2010, **51**, 1485; (c) X. Cai, T. Lei, D. Sun and L. Lin, *RSC Adv.*, 2017, **7**, 15382.